

## COMPARISON OF THE FRACTURE RESISTANCE BETWEEN INLAY RETAINED FIXED PARTIAL DENTURES FABRICATED FROM MILLED PEEK (BIOHPP) AND MONOLITHIC ZIRCONIA (IN VITRO STUDY)

Hesham Ahmed Mostafa <sup>\*</sup> , Noha El-Khodary <sup>\*\*</sup>  and Rasha Sami <sup>\*\*</sup> 

### ABSTRACT

**Aim:** To evaluate the fracture resistance of veneered PEEK Inlay Retained Fixed Partial Dentures (IRFPDs) compared to those fabricated from monolithic zirconia.

**Materials and methods:** Mandibular typodont with removed mandibular first molar was used to receive box inlay cavity preparation on mandibular second molar and second premolar. After tooth preparation, typodont was duplicated into fourteen epoxy models using silicone mold. Epoxy models were randomly divided into two equal groups (n= 7/group). Identical IRFPDs were fabricated from two different materials. For Group I (P/C): IRFPDs were fabricated from Bre. CAM BioHPP blanks and subsequently veneered with composite (Crea.lign). For Group II (MZ): IRFPDs were manufactured using industrially prefabricated monolithic zirconia blocks (Katana HTML). All IRFPDs were bonded to their corresponding epoxy models using adhesive resin cement (Theracem), and underwent thermal cycling (10,000 cycles). Fracture resistance testing was performed on the specimens using a universal testing machine with a crosshead speed of 0.5 mm/min. Fractured samples were examined using a digital-microscope, with 35x magnification power, to determine failure mode pattern.

**Results:** It was found that MZ group recorded statistically significant higher fracture resistance mean value (1876.198±218.039 N) than P/C group (1282.572±160.154 N). Most failures of MZ group were cohesive in nature, where connector fracture was the predominant failure mode. In P/C group, all failures were adhesive in nature between PEEK framework and composite veneering.

**Conclusion:** When compared to Zirconia, PEEK IRFPDs veneered with composite exhibited sufficient resistance to fracture.

**KEYWORDS:** Inlay, fixed partial denture, zirconia, monolithic, PEEK, fracture resistance.

\* Faculty of Dentistry, Future University

\*\* Associate Professor, Fixed Prosthodontic Department, Faculty of Dentistry, Cairo University

## INTRODUCTION

Restorative dentistry major goal is to restore patients' functional and esthetic needs while also ensuring long-term durability and lifespan of the restoration. This critical issue in clinical practice has prompted research into the development of dental materials and clinical procedures capable of accomplishing this goal <sup>(1)</sup>.

Ceramics were first introduced in dentistry when Charles H. Land patented the all-porcelain "jacket" crown in 1989. Since 1989, dental ceramics have progressed significantly, with improvements to their chemical composition, esthetic characteristics, production techniques, packaging, and indications. Early versions of dental ceramics achieved highly esthetic and biocompatible results, but the material's weakness in tensile and shear stresses necessitated the development of ceramic materials with greater strength and durability, especially when thicker restorations are required and/or bonding to dentin is required <sup>(2)</sup>.

Computer Aided Designing/Computer Aided Manufacturing (CAD/CAM) techniques go hand in hand with the ability to press and mill new ceramic restorations, enabling more strong and least invasive ceramic restorations to be fabricated. Understanding the classifications, compositions, and properties of all-ceramic materials have enabled dentists and laboratory technicians to select the most appropriate material for a particular treatment <sup>(3)</sup>. Due to its better flexural strength and fracture toughness when compared to alternative core materials, Yttria-Tetragonal Zirconia Polycrystal (Y-TZP) has recently been deemed the material of choice for posterior all ceramic FPDs <sup>(4)</sup>.

However, a significant disadvantage of bilayered zirconia restorations is the bonding strength between the ceramic veneering and the zirconia core, which is recognized the weakest component of the structure. Monolithic anatomic contoured restorations composed of a single zirconia

layer have been recommended to resolve this problem <sup>(5,6,7)</sup>.

Moreover, numerous surface and internal flaws can operate as stress concentrators, lowering the strength of ceramics. These stresses can result in the formation of cracks, which can then propagate and result in catastrophic failure. Recent years have seen the development of novel materials and processing techniques in an attempt to overcome these fundamental challenges <sup>(8,9)</sup>.

Recently, PolyEtherEtherKetone (PEEK) and its modification BioHPP have been proposed to address the drawbacks of dental ceramics and have been demonstrated to be a viable option for the production of removable partial dentures (RPDs) and FPD frameworks. BioHPP has the same elastic modulus as bone (4GPa), which reduces stresses on the abutment teeth. BioHPP can be used to fabricate frameworks for FPDs, interim restorations following implant insertion, implant abutments, and implant frameworks due to its characteristic physical and mechanical properties. However, due to its natural opaque white hue, it cannot be used as a full contoured restoration in esthetic areas and must be veneered <sup>(10,11)</sup>.

The aggressive full crown preparation required for conventional FPDs may place the pulp vitality at risk, as a significant portion of the coronal tooth structure must be removed. On the other hand, conservative procedures such as inlay-retained fixed partial dentures (IRFPDs) have been proposed for replacing posterior single missing teeth. IRFPDs utilize box-shaped preparation forms as retainers and may incorporate existing fillings on adjacent teeth <sup>(1,12)</sup>.

The introduction of adhesives in dentistry has increased restoration retention, improved cosmetic results, and lowered invasiveness in disciplines of prosthetic and restorative dentistry. When minerals are removed from hard tissues, resin monomers are substituted, and the resin forms a hybrid layer

of bonding or micromechanical interlocking. Various adhesion processes, different materials, and substrate preparation procedures capable of affecting the degree of adhesion have been investigated throughout the years<sup>(13)</sup>.

Therefore, our goal in this study was to compare between the fracture resistance of inlay retained fixed partial dentures fabricated from CAD/CAM milled PEEK frameworks and veneered with composite, and monolithic zirconia inlay retained fixed partial dentures, after thermocycling. The null hypothesis was that there will be no difference in fracture resistance between PEEK IRFPD frameworks veneered with indirect composites and those fabricated from monolithic zirconia.

## MATERIALS AND METHODS

### Teeth preparation on typodont

A special partially edentulous mandibular typodont (Nissin dental products INC., Kyoto, Japan) was selected. Mandibular left first molar was removed from the typodont and inlay cavities on the second premolar and second molar were prepared adjacent to the pontic space. Teeth preparations were done according to the recommended dimensions for all ceramic inlay retained fixed partial denture with a parallelometer device (Nouvag AF 30, Goldach, Switzerland), to standardize the cavity preparation dimensions<sup>(14)</sup>.

The second premolar received disto-occlusal inlay cavity preparation as follow:

The occlusal part was prepared with 2 mm depth from the central groove, 2 mm bucco-lingual width (approximately one third the inter-cuspal width), and 3mm mesiodistally.

The proximal box was prepared with 2 mm depth from the level of the pulpal floor to the gingival seat, 3.5 mm bucco-lingually, and 1.5 mm mesiodistally.

The second molar received mesio-occlusal inlay cavity preparation as follow:

The occlusal part was prepared with 2mm depth from the central groove, 3mm buccolingual width (nearly one third the inter-cuspal width), and 4mm mesiodistally.

The proximal box was prepared with 2 mm depth, 5 mm buccolingual, and 1.5 mm mesiodistal.

Dimensions were measured with a periodontal probe. Cavo-surface margins were finished in butt joint with no bevels. Taper was 6° from the depth of the cavity to the cavo-surface margin. All internal line angles were made rounded and smooth.

### Epoxy models fabrication

The area of missing first molar was filled with wax, making an edentulous contour. Typodonts were duplicated to epoxy resin models of high strength\*. A silicone mold\*\* was fabricated over the typodont into which the epoxy resin mixture was poured to fabricate 14 epoxy models. Models were randomly divided into two groups ( n=7 samples/group).

For group I (P/C) : IRFPDs manufactured using industrially prefabricated Bio-Hpp veneered with the composite, while for Group II (MZ): IRFPDs manufactured using industrially prefabricated monolithic zirconia blocks.

### Scanning of epoxy resin models

To obtain three dimensional images of epoxy resin models for both groups, an extraoral scanner\*\*\* which is based on structured light scanning technology was used. Scanning was repeated the same way for all epoxy resin models and STL file for each model was created and exported to the computer to start the designing procedures of the IRFPDs

\* Kemapoxy 150, Chemical Industries of Construction CIC-Egypt,

\*\* Replisil 22 N, SILCONIC® GmbH & Co. KG, Münster Germany

\*\*\* D Scan 5, EGSolutions, Italy

## Construction of CAD/CAM milled IRFPDs

### Group I: (P/C)

The scanned STL files were individually used by one experienced dental technician using exocad dental CAD software\* to design the framework of IRFPDs. Mesial and distal cavity preparation dimensions were verified with the software. Margins of the mesial and distal inlay retainers were then identified. The framework thickness of the mesial and distal inlay retainers was designed according to the recommended values by the manufacturer to be approximately 1mm thickness, which provided the required space for veneering composite to be 1mm thickness as adopted by (11). Sanitary pontic was virtually designed on the software with 2 mm space between the gingival portion of the pontic and the model. Pontic span length was set at 11mm approximately. The connector dimensions were set to be (3.5mm\*4mm) as recommended by the manufacturer, and the cement gap was defined as 50 $\mu$ , measured 0.05mm from the defined margins.

After framework designing; STL files were sent to the milling unit\*\* software, Bre.CAM BioHPP PEEK blank type (98.5 mm diameter and 12 mm fold) was selected and milled using milling burs\*\*\* especially matched with the properties of the material, with 0.6 mm, 1 mm and 2 mm diameter. After milling, the frameworks were detached from the mill connectors, and visually checked over their corresponding epoxy models for verification of proper. Samples with gross discrepancies were discarded and replaced by newly fabricated samples.

The frameworks were airborne-particle abraded in a pneumatic micro sandblaster with 110 Al<sub>2</sub>O<sub>3</sub>\*\*\*\* powder particles with 0.25 MPa, at 45° angle from

an average distance of 10 mm. Any impurities were then removed using alcohol and a clean brush, according to the manufacturer.

Following that, frameworks were conditioned with visio.link adhesive applied in a thin coating using special painting brush\*\*\*\*\* and immediately polymerized for 90 seconds (intensity: 220 mW/cm<sup>2</sup>) in special light curing device\*\*\*\*\*. For mechanical retentions, the dual-hardening combo.lign wash opaquer was applied over the frameworks as the first layer to mask the grayish color of PEEK, and polymerized for 180 seconds in the same light curing device. Following light curing, the frameworks appeared with a semi-matt finish, ensuring uniform layer thickness of wash opaquer. Crea.lign opaquer was then applied to provide the required masking of the framework color, and light polymerized for 180 seconds. The mat surface obtained after polymerizing was an indicator for proper curing.

To standardize the veneering composite thickness and contour, a transparent silicone index was fabricated over one of the milled and finished fully contoured monolithic zirconia IRFPDs, served as the master model for the silicon mold. The fabricated silicone index was then checked for perfect fit over the PEEK epoxy models to ensure complete seating. After that, crea.lign veneering composite was applied over the PEEK frameworks seated on their corresponding epoxy models and inside the silicone index, and then light cured through the transparent silicone index for 180 seconds in the light curing device. The restorations were then finished and polished using PEEK polishing kit\*\*\*\*\*. After polishing, fabricated samples were then seated over their corresponding models, being ready for the cementation procedures *Figure (1)*.

\* Exocad GmbH, Germany

\*\* Shera eco mill 5X, Shera Werkstoff Technology, Germany

\*\*\* Primadigital fit for Vhf, UK

\*\*\*\* Oxyker duet, Manfredi, Italy

\*\*\*\*\* Crea.lign veneering toolkit, Bredent, UK

\*\*\*\*\* Bre.lux power unit, Bredent, UK

\*\*\*\*\* visio.lign® Polishing Toolkit, Bredent, UK



Fig. (1) P/C sample



Figure (2): MZ sample

### Group II: MZ

The scanned STL file was used by exocad software to design a full contoured IRFPD. Cavity preparation dimensions were verified with the software, and the margins were identified, as for group 1. The mesial and distal connector dimensions were selected to be 3\*3 mm. The cement gap was selected to be 50 $\mu$ , measured 0.5mm from the margins.

After all zirconia IRFPDs were milled (dry milling), a finishing bur was used to separate the restorations from the blocks, finishing burs were used to produce smoother finished surface.

Samples were then sintered as recommended by the manufacturer in a sintering furnace\*. The cycles had approximately taken seven hours to be terminated. Glazing was carried out using Clear Glaze\*\* paste applied with special brush, then went glazing cycle\*\*\* according to the manufacturer instructions. After the glazing cycle had been terminated, all specimens were visually checked over their models to ensure proper fit, as done for group I *Figure (2)*.

\* ARROW furnace, Dentas, Slovenia

\*\* Cerabian ZR Clear Glaze, FC Paste stain, Noritake, Japan

\*\*\* Summit Press, IBEX Dental Technologies, USA

### Cementation

#### Group I: P/C

For P/C group, the cementation surfaces of inlay retainers were abraded with 110  $\mu$  Al<sub>2</sub>O<sub>3</sub> particles, cleaned with distilled water in an ultrasonic unit, and gently air dried with oil free air stream. For MZ group, IRFPDs were sandblasted with 110 $\mu$  Al<sub>2</sub>O<sub>3</sub> at a maximum pressure of 1 bar for 10 seconds from 1cm distance<sup>(15)</sup>. The internal surfaces of the restorations were cleaned with distilled water in an ultrasonic unit, rinsed, and dried. One or two coats of Z-prime plus were applied, wetting the bonding surfaces uniformly and then dried with an air syringe for 5 seconds.

Theracem self-adhesive resin cement was then dispensed directly into the epoxy models using an endo tip. Restorations were first placed in site with a finger pressure; A loading device was then used for the application of a uniform load of 3 kg (30 N) for 10 minutes over the cemented restorations along the longitudinal axis of the pontic to ensure proper cementation till cement polymerization. A rubber sheet was placed between the load and the occlusal surface of the pontic to prevent direct contact and possible cracking. After initial curing and removal of excess cement, a prolonged light-curing was performed from mesio-buccal, mesio-palatal, disto-buccal, disto-palatal and occlusal directions for 40 seconds each.

### Thermocycling

The cemented restorations were then stored in distilled water at 37°C for 24 hours and then underwent thermocycling (10,000 cycles  $\times$  5–55°C) in a thermocycling apparatus\*. Dwell time was 25 (sec). in each water bath and lag time was 10 (sec).

### Fracture resistance testing

Each sample was individually mounted on a computer-controlled universal testing machine\*\* equipped with a 5 kN load cell, and data were collected using computer software\*\*\*. Screws were employed to secure samples to the testing machine's lowest fixed compartment. The fracture test was conducted using a metallic rod with a spherical tip (3.8 mm diameter) connected to the testing machine's upper movable compartment, moving at a cross-head speed of 1mm/min and separated by a thin tin foil sheets to ensure uniform stress distribution and minimize local load transmission. An audible crack indicated the load at failure, which was verified by a sharp decrease in the load-deflection curve measured using the computer software. The force necessary to fracture was quantified in Newtons.

### Fractographic analysis

Following the fracture resistance test, all fractured samples were viewed with a USB digital microscope equipped with a 35x magnification power. To detect the failure mode pattern, images were captured and transmitted to an IBM computer, equipped with the Image-tool program.

## RESULTS

All data were collected and analyzed using Graph Pad InStat (Graph Pad, Inc.) software. Data were presented as mean, standard deviation (SD)

\* Robota automated thermal cycle; BILGE, Turkey

\*\* Instron Industrial Products, Model 3345, Norwood, MA, USA

\*\*\* Instron® Bluehill Lite Software

for values. A value of  $P \leq 0.05$  was considered statistically significant. After homogeneity of variance and normal distribution of errors had been confirmed, student t-test was done for comparison. Chi square test was performed between failure mode patterns. Sample size ( $n=7$ ) was large enough to detect large effect sizes for main effects and comparisons, with the satisfactory level of power set at 80% and a 95% confidence level<sup>(16,17)</sup>.

### Fracture resistance

For **P/C** group the mean  $\pm$  SD values were (1282.572 $\pm$ 160.154 N) with minimum value (971.63 N) and maximum value (1507.19 N), while for **MZ** group the mean  $\pm$  SD values were (1876.198 $\pm$ 218.039 N) with minimum value (1630.51N) and maximum value (2341.38 N). It was found that **MZ** group recorded statistically significant higher mean fracture resistance value than **P/C** group as tested by un-paired t-test ( $p = 0.0002 < 0.05$ ) **Table (1) and Figure (3)**.

### Failure modes

Frequent distribution of failure mode scores (%) for both groups were summarized in **table (2)** and graphically drawn in **Figure (4)**.

The difference in frequent distribution of failure modes scores between both groups was statistically significant as indicated by chi square test ( $P = < 0.0001 < 0.05$ )

**P/C** group showed adhesive failure mode pattern (favorable) in all samples **Figure (5.a)** with no record for cohesive or mixed failure mode patterns (non-favorable). In **MZ** group, the failure mode pattern was predominantly cohesive **Figure (5.b)** while minority was mixed (non-favorable) **Figure (5.c)**, with no record for adhesive failure mode pattern (favorable).

TABLE (1) Descriptive statistics of fracture resistance test results (Mean±SD) for both material groups after thermal aging (N)

Variables	Descriptive statistics						t-test	
	Mean±SD	Range		95% confidence intervals		t-value	P value	
		Min.	Max.	Lower	Upper			
Material group	<b>P/C</b>	1282.572±160.154	971.63	1507.19	1163.931	1401.213	5.4	0.0002*
	<b>MZ</b>	1876.198±218.039	1630.51	2341.38	1714.675	2037.72		

\*Significant (p<0.05)

TABLE (2) Frequent distribution of failure modes scores (%) for both groups

Material group	Failure mode	Failure mode			Statistics	
		Favorable	Non-favorable		Chi-value	P value
		Adhesive	Cohesive	Mixed		
PEEK	Zr	7 (100%)	0 (0%)	0 (0%)	107	<0.0001*
	Zr	0 (0%)	6 (85.71%)	1 (14.29%)		

\*; significant (p<0.05)

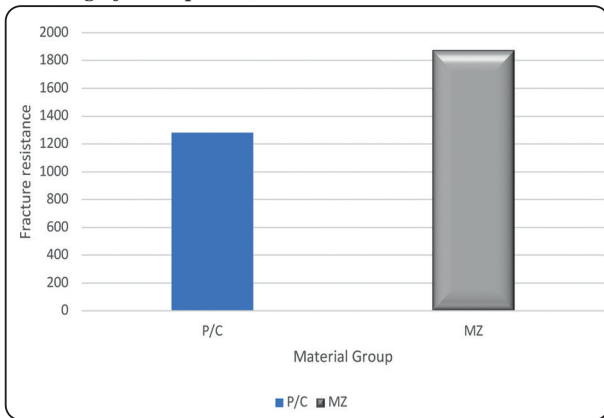


Fig. (3) Column chart comparing the mean values of fracture resistance for both groups after thermal aging

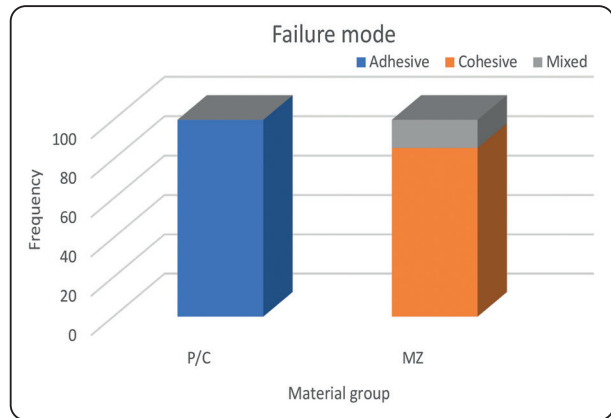


Fig. (4): Stacked column chart comparing the frequent distribution of failure modes scores for both groups

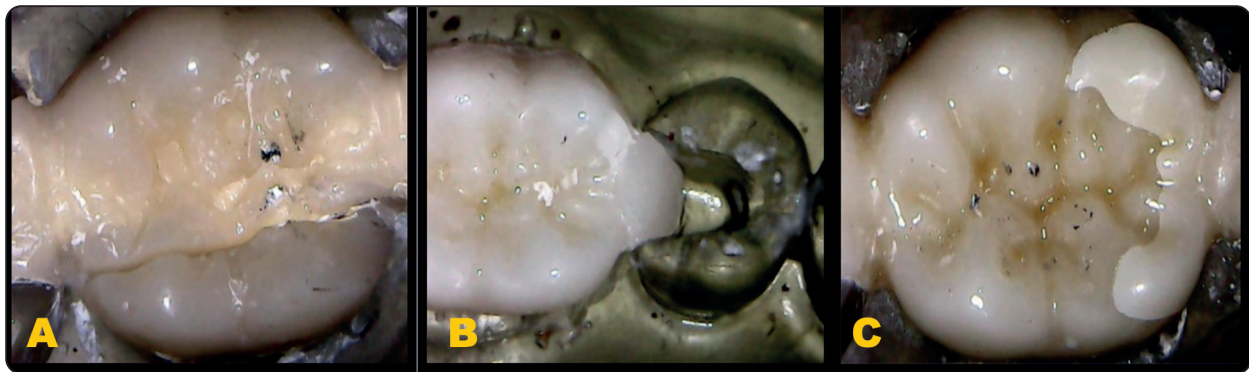


Fig. (5): (a) digital microscopic image showing favorable failure mode pattern in P/C group. (b) digital microscopic images showing non-favorable isthmus fracture in MZ group. (c) digital microscopic images showing non-favorable connector fracture in MZ group.

## DISCUSSION

In this study, we aimed to test the fracture resistance of PEEK as a new evolving material, and compare the results with zirconia. Before suggesting a new material for clinical application, it is necessary to compare the results of in-vitro tests to those of recognized and accepted materials <sup>(10)</sup>.

Standardized three-unit IRFPDs were used to imitate clinical settings in the current investigation rather than simple bars, because the dimensions and forms of IRFPDs are quite different from those of bars, does not account for the effect of the complicated geometry of dental restorations <sup>(8)</sup>.

Instead of metal models, epoxy models were used in our study to conduct the fracture resistance test since they have an elastic modulus similar to that of natural teeth. It was demonstrated that the elastic modulus of the abutment material has an effect on the fracture resistance of all-ceramic restorations <sup>(12)</sup>.

To eliminate variable factors and ensure homogeneity of results in the current investigation, "typodont teeth" were prepared by the same operator using a parallelometer device and then duplicated.

Each epoxy resin model was scanned to confirm accurate seating of the restorations over their corresponding models, which was in agreement with *Gumus et al (2018)* <sup>(5)</sup> and *AlAssar et al. (2017)* <sup>(17)</sup>.

Additionally, the identical form of all samples ensured identical stress conditions, as varied IRFPD geometries can result in diverse fracture patterns. To assure virtually similar samples and to standardize veneering composite thickness, a silicone mold was created over one of the full anatomic machined zirconia IRFPDs and utilized for veneering the PEEK frameworks, as in agreement with *Wolfart et al. (2007)* <sup>(15)</sup> and *Nagas et al. (2018)* <sup>(11)</sup>.

IRFPDs were cemented to their individual epoxy models to accurately mimic the clinical situation and

to prevent any little movement of the restorations during the fracture test from affecting the study results.

All specimens were thermocycled (10,000 cycles, 5°C-55°C, 20-second intervals) to simulate one year of intra-oral conditions, as previously reported by *Gumus et al (2018)* <sup>(5)</sup>, and *Schwitalla et al. (2015)* <sup>(18)</sup>.

The fracture force was applied using a steel ball to eliminate any interference with the cusp height that could alter the results. A uniform layer of tin foil was placed between the occlusal surface of the samples and the steel ball to prevent any direct contact that could result in uneven stress distribution. Cusp morphology and its effect on failure types warrant further investigations.

It was found that *MZ* group recorded statistically significant higher fracture resistance mean value (1876.198±218.039 N) than *P/C* group (1282.572±160.154 N). Accordingly, the null hypothesis was rejected.

Regarding *P/C* group, our results were in consistence with *Nagas et al. (2018)* <sup>(11)</sup>, who reported that PEEK IRFPDs veneered with composite have mean load bearing capacity of (995.5±78.1N), and contradicting to *Al Assar et al. (2017)* <sup>(17)</sup>, who stated that PEEK IRFPDs had a lower fracture resistance (600 N for BioHPP granules and 684 N for BreCAM BioHPP), which could be attributed to cementing samples to natural teeth, rather than epoxy models.

Results of *MZ* group were comparable to *Mehl et al. (2010)* <sup>(19)</sup>, who reported similar fracture resistance values for zirconia IRFPDs (1749N) when centric load was applied. Because of the transformation-toughening mechanism of zirconia, frameworks offer remarkable fracture strength. However, due to variations in study methodology and materials used, direct correlation between results was difficult.

In contradiction to our results, **Wolfart et al. (2007)** <sup>(15)</sup> reported much higher fracture resistance values for zirconia veneered IRFPDs (3180N). They related their results to the mechanical properties of zirconia, and the stiffness of the metal abutment used in their study, because of the different modulus of elasticity of Co–Cr alloy (180–240 GPa), compared to natural teeth (50–85 GPa for enamel, and 15–20 GPa for dentin). Contrary to our results, **Kermanshah et al. (2020)** <sup>(20)</sup> and **Mohsen et al. (2010)** <sup>(21)</sup> reported lower fracture resistance of monolithic zirconia IRFPDs. **Kermanshah et al.** attributed this significant variation in results to the box shaped cavity preparation design since limited surface area was available for bonding, compared to occluso-proximal box preparation. They also attributed their lower results to the total occlusal convergence (20°) as increasing preparation tapers inversely influenced the fracture resistance of all-ceramic inlays. Moreover, they bonded the restorations to natural teeth instead of epoxy models.

The failure pattern analysis revealed that all PEEK IRFPDs demonstrated interfacial fracture in the pontic veneering composite. All fractures between the PEEK framework and the opaquer veneering composite were adhesive in nature, with no complete fracture of the framework. These fracture patterns were comparable to those observed in bi-layered metal ceramic IRFPDs <sup>(22)</sup>, and lithium disilicate veneered zirconia FPDs <sup>(10)</sup>. This observation was also consistent with the findings of **Ozcan et al (2005)** <sup>(23)</sup>, who described veneering resin cracking and chipping as a two-phase failure pattern followed by adhesive failure between the veneering resin and the framework.

The adhesive fracture pattern could be related to the decrease in bond strength caused by thermocycling and the development of cracks in the veneering composite near the connector area. Similarly, **Stawarczyk et al. (2015)** <sup>(24)</sup> found that during thermocycling, cracks in the veneering

composite resin occurred regardless of the pretreatment, type of adhesive applied, or composite resin veneering utilized.

The observed pure adhesive failure was due to the pretreatment. While the airborne particle abrasion greatly increases and facilitates the infiltration of the adhesive material, the bonding process is still primarily defined by mechanical interlocking between the PEEK substrate and the adhesive material. In comparison, the veneering composite is chemically bonded to the adhesive visio.link layer, resulting in a stronger bond in all circumstances examined in this study.

*This failure mode of P/C group was in contradiction to Nagas et al. (2018)* <sup>(11)</sup> and **Jin et al. (2019)** <sup>(25)</sup>, who reported that PEEK restorations fractured at the connector site. Due to the variability of the materials used from different manufacturers, direct comparison was difficult.

On the other hand, Z- IRFPD specimens displayed different fracture patterns. one specimen demonstrated fracture of mesial retainer at the isthmus portion - the connection between the occlusal part and the proximal box of the inlay-. The remaining samples demonstrated cohesive fracture of either the mesial or distal connector.

Cohesive failure of monolithic zirconia was related to thermomechanical fatigue This was explained by zirconia susceptibility to Low Temperature Degradation (LTD), which is primarily initiated in moist conditions. In accordance with **Partiyan et al. (2017)** <sup>(26)</sup> and **Gumus et al. (2018)** <sup>(5)</sup>, the stress concentration on the connector tensile surface (cervical surface), along with the influence of fatigue, surface degradation, and insufficient connector height, are responsible for increasing the likelihood of fracture during function. These studies reported similar connector fractures of monolithic zirconia IRFPDs cemented to epoxy models. These characteristic fracture lines have been found in previous research as well <sup>(15,22)</sup>.

Along with subcritical crack growth (SCG) caused by chemical deterioration, another component that contributes to dental ceramics fracture is mechanical fatigue, which occurs primarily during cyclic loading and cannot be predicted from static or monotonic loading tests -as in our study-. Mechanical fatigue is a relatively destructive process, which means that calculations solely based on -load to fracture- assumptions may significantly overestimate probable lifetimes.

Monolithic zirconia is more fracture resistant than its PEEK/C counterpart when employed in IRFPDs. Both materials, however, resisted mechanical fracture loads greater than the usual occlusal forces delivered clinically in the posterior region, agreeing with *Jin et al. (2019)*<sup>(25)</sup> and *Taufall et al. (2016)*<sup>(27)</sup>.

One limitation in our study is that no mechanical loading was applied as part of the artificial ageing process, which would have a detrimental influence on the investigated materials. Another limitation was that loading in vitro is likely to differ from loading under clinical conditions, where masticatory forces work both axially and non-axially.

## CONCLUSIONS

**Within the limitations of the present study, the following could be concluded:**

- BioHPP might have significant advantages for dental applications because of high fracture resistance and better stress distribution.
- Being a brittle material, connector fracture was the predominant failure mode of monolithic zirconia IRFPDs.
- The weakest part of veneered BioHPP was the interface between framework and veneering material where adhesive failure predominantly occur.

## RECOMMENDATIONS

- Thermo- mechanical fatigue tests are important to simulate the oral conditions
- Conducting fracture resistance testing on samples cemented to natural teeth to simulate clinical conditions.

## REFERENCES

1. Edelhoff, Daniel, and John A. Sorensen. (2002). "Tooth Structure Removal Associated with Various Preparation Designs for Posterior Teeth." *International Journal of Periodontics and Restorative Dentistry* 22(3): 241–50.
2. Kelly, J. R., and Benetti, P. (2011). "Ceramic materials in dentistry: Historical evolution and current practice." *Australian Dental Journal*. 56(Suppl 1): 84–96
3. Koch, George K., German O. Gallucci, and Sang J. Lee. (2016). "Accuracy in the Digital Workflow: From Data Acquisition to the Digitally Milled Cast." *Journal of Prosthetic Dentistry* 115(6): 749–54.
4. Beuer F, Schweiger J, Edelhoff D. Digital dentistry: an overview of recent developments for CAD/CAM generated restorations. *Br Dent J*. 2008 May 10;204(9):505-11.
5. Hilal Siriner Gumus , Nilufer Tulin Polat, Guler Yildirim. (2018). "Evaluation of Fracture Resistance of Inlay-Retained Fixed Partial Dentures Fabricated with Different Monolithic Zirconia Materials." *J Prosthet Dent* . 119(6): 959–64.
6. Preis, Verena et al. (2012). "In Vitro Failure and Fracture Resistance of Veneered and Full-Contour Zirconia Restorations." *Journal of Dentistry* 40(11): 921–28.
7. Lameira, Deborah Pacheco, Wilkens Aurélio Buarque E. Silva, Frederico Andrade E. Silva, and Grace M. De Souza. (2015). "Fracture Strength of Aged Monolithic and Bilayer Zirconia-Based Crowns." *BioMed Research International* 2015.
8. Aboushelib, Moustafa N., Niek de Jager, Cornelis J. Kleverlaan, and Albert J. Feilzer. (2007). "Effect of Loading Method on the Fracture Mechanics of Two Layered All-Ceramic Restorative Systems." *Dental Materials* 23(8): 952–59.
9. Babu, P. Jithendra et al. (2015). "Dental Ceramics: Part I – An Overview of Composition, Structure and Properties." *American Journal of Materials Engineering and Technology* 3(1): 13–18.

10. Choi, Jae Won et al. (2017). "In Vitro Study of the Fracture Resistance of Monolithic Lithium Disilicate, Monolithic Zirconia, and Lithium Disilicate Pressed on Zirconia for Three-Unit Fixed Dental Prostheses." *Journal of Advanced Prosthodontics* 9(4): 244–51.
11. Cekic-Nagas, Isil et al. (2018). "Load-Bearing Capacity of Novel Resin-Based Fixed Dental Prosthesis Materials." *Dental Materials Journal* 37(1): 49–58.
12. Saridag, Serkan, Atilla Gokhan Ozyesil, and Gurel Pekkan. (2012). "Fracture Strength and Bending of All-Ceramic and Fiber-Reinforced Composites in Inlay-Retained Fixed Partial Dentures." *Journal of Dental Sciences* 7(2): 159–64.
13. Russo, Daniele Scaminaci, Francesca Cinelli, Chiara Sarti, and Luca Giachetti. (2019). "Adhesion to Zirconia: A Systematic Review of Current Conditioning Methods and Bonding Materials." *Dentistry Journal* 7(3).
14. Thompson, M. C., K. M. Thompson, and M. Swain. (2010). "The All-Ceramic, Inlay Supported Fixed Partial Denture. Part 1. Ceramic Inlay Preparation Design: A Literature Review." *Australian Dental Journal* 55(2): 120–27.
15. Wolfart, Stefan, Klaus Ludwig, Anja Uphaus, and Matthias Kern. (2007). "Fracture Strength of All-Ceramic Posterior Inlay-Retained Fixed Partial Dentures." *Dental Materials* 23(12): 1513–20.
16. Faul, Franz, et al. "G\* Power 3: A flexible statistical power analysis program for the social, behavioral, and biomedical sciences." *Behavior research methods* 39.2 (2007): 175-191
17. Al Assar, Roqaia, Mohammed Al yasky, Mona Mandour, and Rania Amin. (2017). "Fracture Resistance and Retention of Metal-Free Inlay Retained Fixed Partial Dentures." *Al-Azhar Dental Journal for Girls* 4(4): 395–407.
18. Schwitalla, Andreas, Tobias Spintig, Iona Kallage, and Wolf-Dieter Müller-Müller. (2015). "Flexural behavior of PEEK materials for dental application." *Dental Materials*(1).Pdf."
19. Mehl, Christian, Klaus Ludwig, Martin Steiner, and Matthias Kern. (2010). "Fracture Strength of Prefabricated All-Ceramic Posterior Inlay-Retained Fixed Dental Prostheses." *Dental Materials* 26(1): 67–75.
20. Kermanshah, Hamid, Fariba Motevasselian, Saeedeh Alavi Kakhaki, and Mutlu Özcan. (2020). "Effect of Ceramic Material Type on the Fracture Load of Inlay-Retained and Full-Coverage Fixed Dental Prostheses." *Biomaterial Investigations in Dentistry* 7(1): 62–70.
21. Mohsen, Cherif A. (2010). "Fracture Resistance of Three Ceramic Inlay-Retained Fixed Partial Denture Designs. An in Vitro Comparative Study." *Journal of Prosthodontics* 19(7): 531–35.
22. Kiliçarslan, Mehmet A., P. Sema Kedici, H. Cenker Küçükşemen, and Bülent C. Uludağ. (2004). "In Vitro Fracture Resistance of Posterior Metal-Ceramic and All-Ceramic Inlay-Retained Resin-Bonded Fixed Partial Dentures." *Journal of Prosthetic Dentistry* 92(4): 365–70.
23. Ozcan, Mutlu, Marijn H. Breuklander, and Pekka K. Vallittu. (2005). "The Effect of Box Preparation on the Strength of Glass Fiber-Reinforced Composite Inlay-Retained Fixed Partial Dentures." *Journal of Prosthetic Dentistry* 93(4): 337–45.
24. Stawarczyk, Bogna, Marlis Eichberger, et al. (2015). "Three-Unit Reinforced Polyetheretherketone Composite FDPs: Influence of Fabrication Method on Load-Bearing Capacity and Failure Types." *Dental Materials Journal* 34(1): 7–12.
25. Jin, Hang ying et al. (2019). "Comparative Evaluation of BioHPP and Titanium as a Framework Veneered with Composite Resin for Implant-Supported Fixed Dental Prostheses." *Journal of Prosthetic Dentistry* 122(4): 383–88.
26. Partiyani, Arthur et al. (2017). "Fracture Resistance of Three-Unit Zirconia Fixed Partial Denture with Modified Framework." *Odontology* 105(1): 62–67.
27. Tauffall, Simon, Marlis Eichberger, Patrick R. Schmidlin, and Bogna Stawarczyk. (2016). "Fracture Load and Failure Types of Different Veneered Polyetheretherketone Fixed Dental Prostheses." *Clinical Oral Investigations* 20(9): 2493–2500.